J Radioanal Nucl Chem
DOI 10.1007/s10967-012-2045-y

Optimization of a prompt gamma setup for analysis of environmental samples

A. A. Naqvi · Faris A. Al-Matouq · F. Z. Khiari · Khateeb-ur-Rehman · M. A. Gondal · A. A. Isab

Received: 17 July 2012

Abstract A thermal neutron capture-based Prompt Gamma ray Activation Analysis setup has been designed to analyze the elemental concentration of environmental bulk samples using a D(d,n) reaction-based portable neutron generator. The performance of the setup was tested through mercury concentration measurements in Hg-contaminated water samples using a large volume cylindrical bismuth germinate (BGO) gamma ray detector. Excellent agreement of experimental count rate of 2.64, 3.19 + 3.29 and 4.67–5.05 MeV Hg prompt gamma rays with theoretical count rate obtained through Monte Carlo simulations, indicates excellent performance of the newly designed portable neutron generator-based PGNAA setup.

Keywords Prompt gamma neutron activation analysis · Hg contaminated bulk water samples · Prompt gamma ray yield measurements · PGNAA setup design calculations using Monte Carlo calculations · Comparison of experimental and calculation results

Introduction

Prompt Gamma-ray Neutron Activation Analysis (PGNAA) technique is widely used for in situ elemental analysis of bulk samples in several scientific disciplines including environmental, industrial and health sciences [1–5]. Its area of application ranges from quality-control tasks in mining, manufacturing and building construction industries [5, 6] to contraband detection for homeland security [7]. In conjunction with radioisotope neutron sources [4] and portable neutron generators [5, 8], PGNAA technique can be extended to in situ prompt gamma-ray analysis of environmental and biological bulk samples [9–13]. PGNAA technique is ideally suited for concentration measurements of elements with high thermal neutron capture cross section. Then the resulting detection sensitivity of the PGNAA technique for the specific element is high as compared to other bulk sample analysis techniques. Mercury (Hg) has large thermal neutron capture cross section. For example production cross section of 386 keV Hg gamma ray is 251 barns.

King Fahd University of Petroleum and Minerals (KFUPM), Dhahran, Saudi Arabia, has acquired a portable D–D reaction-based pulsed neutron generator model MP320, from Thermo-Fisher, USA, for the elemental analysis of bulk samples [5].A PGNAA setup has been developed for thermal neutron capture-based prompt gamma ray analysis utilizing the portable neutron generator. In order to optimize the design of the moderator of the PGNAA setup, the thermal neutron flux at the sample location was calculated for three different source-moderator-sample geometries. Finally, the PGNAA setup was fabricated using the moderator design with maximum count rate of thermal neutron flux at the sample location. Due to the smaller thermal neutron flux available at the portable neutron generator, an element with high thermal neutron capture cross section such as Hg (251 barn production cross section for 386 keV Hg gamma ray) was used to test the response of the PGNAA setup. The performance of the PGNAA setup was then tested through prompt gamma-ray analysis of mercury-contaminated bulk water

A. A. Naqvi (✉) · F. A. Al-Matouq · F. Z. Khiari · Khateeb-ur-Rehman · M. A. Gondal
Department of Physics, King Fahd University of Petroleum and Minerals, Dhahran, Saudi Arabia
e-mail: aanaqvi@kfupm.edu.sa

A. A. Isab
Department of Chemistry, King Fahd University of Petroleum and Minerals, Dhahran, Saudi Arabia

Published online: 10 August 2012

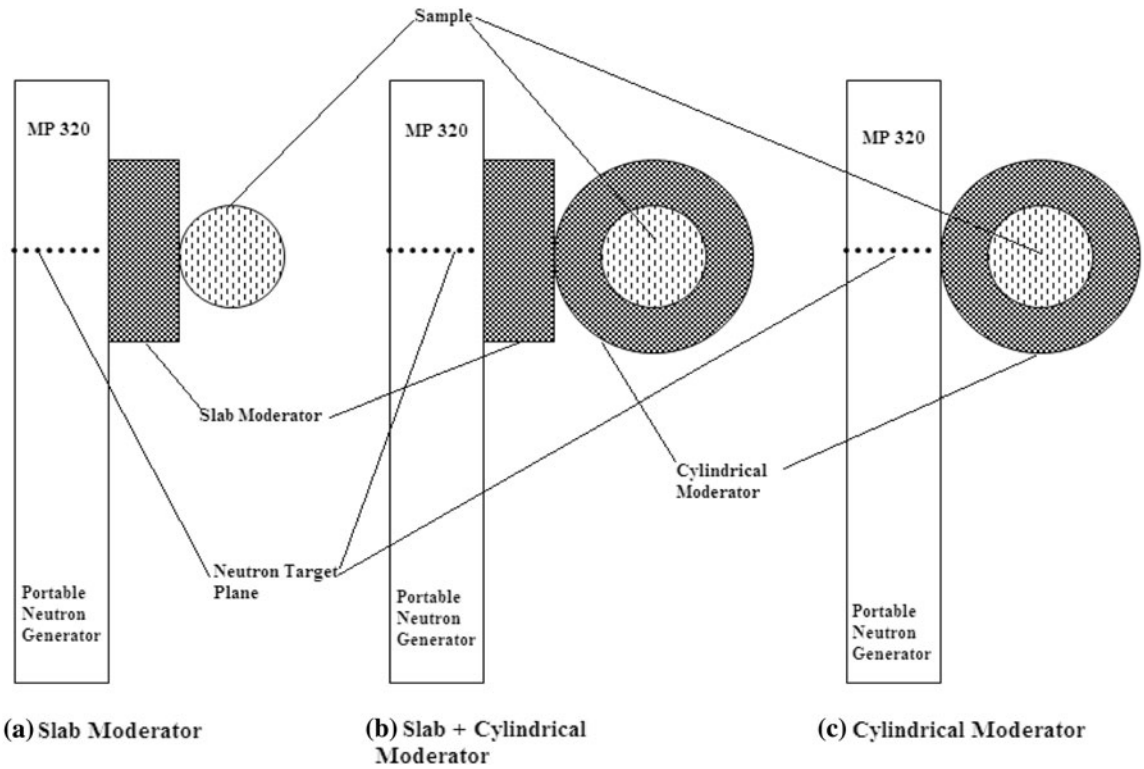

Fig. 1 Top view of schematic of three different source-moderator-sample geometries of PGNAA setup tested in the present study

samples. In the following text the study is described in detail.

Experimental

Design calculations of moderator of portable neutron generator-based PGNAA setup

Monte Carlo calculations were carried out using code MCNP4B2 [14] to design a portable neutron generator-based PGNAA setup following the procedure published earlier [5]. In order to optimize the source-moderator-sample geometry of the setup, the thermal neutron flux at the sample location was calculated for three different arrangements of source-moderator-sample geometry as shown in Fig. 1a–c. Figure 1a shows the geometry for thermal neutron flux production at a cylindrical sample (90 mm in diameter and 145 mm in height)by inserting cylindrical high density polyethylene (HDPE) moderator slab between the neutron target of the portable neutron generator and the sample (standing in upright position). The cylindrical HDPE moderator slab (disk shaped) has a fixed 25 cm diameter. The moderator disk thickness was varied in one-cm steps by keeping the moderator diameter and sample volume fixed and changing the sample position with respect to the source. The thermal neutron count rate was calculated in the sample volume for each slab moderator thickness. In the next step, as shown in the configuration of Fig. 1b, the sample was enclosed in a HDPE moderator cylinder and was placed after a cylindrical HDPE slab-moderator with 6 cm thickness obtained from calculations of part (a) corresponding to Fig. 1a. The cylindrical slab was included again in the geometry to find neutron beam-focusing effects of the slab on the cylindrical moderator, if any. In part (b) of this study, corresponding to Fig. 1b, the outer diameter of the cylinder (moderator thickness around the sample) was varied in equal steps and the thermal neutron count rate was calculated in the sample volume for each external diameter of the HDPE cylinder. Finally, the sample was enclosed in a HDPE cylinder and was placed next to the neutron target without the slab, as shown in Fig. 1c. The thermal neutron count rate was calculated in the sample volume as a function of the HDPE cylinder outer diameter (moderator thickness around the sample).

Figure 2 shows the calculated thermal neutron count rate as a function of moderator thickness for the three different cases superimposed upon each other for comparison purpose. The thermal neutron count rate for slab-moderator case (Fig. 1a) increases with moderator thickness and reaches an optimum value for 6 cm thick slab-moderator and then drops off due to the increasing distance from the

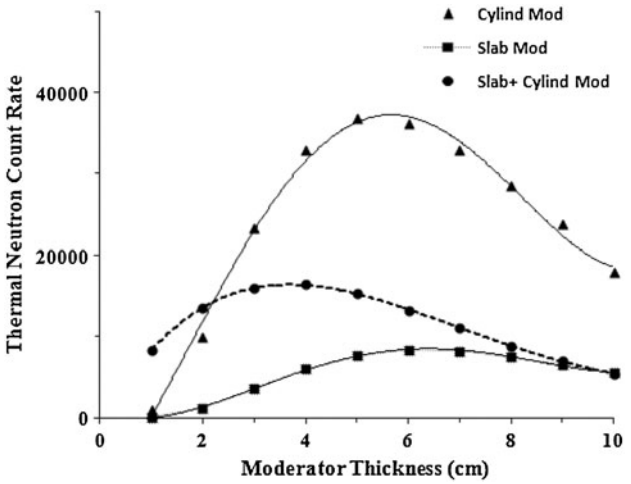

Fig. 2 Thermal neutron count rate at the sample location from the three geometries plotted as the effective moderator thickness

neutron source. By further enclosing the sample in a cylindrical moderator, the thermal neutron count rate increases with increasing thickness of the cylinder outer diameter (moderator thickness around the sample) and then decreases. The maximum count rate of thermal neutrons in slab + cylinder case was obtained for a combination of 6 cm thick slab-moderator and 4 cm thick HDPE cylinder around the sample.

Figure 2 also shows the thermal neutron count rate for the sample enclosed in the HDPE cylindrical moderator without the slab in Fig. 1c. The count rate increases with cylinder thickness till it reaches a maximum value for 6 cm thick HDPE cylinder. With further increases in thickness of the cylinder moderator, the thermal neutron intensity decreases, a trend similar to the ones observed in Fig. 1a and b. The thermal neutron intensity obtained in the design of part (c) was two times higher than the best value achieved from part (a) and (b) designs. Therefore, the design of part (c) was adopted to fabricate the moderator of the portable neutron generator-based PGNAA set.

Figure 3 shows a schematic of the complete portable neutron generator-based PGNAA setup. The PGNAA setup consists of a cylindrical specimen container placed in a cylindrical cavity drilled through a cylindrical HDPE moderator. A cylindrical gamma-ray detector, with its longitudinal axis aligned along the sample's longitudinal axis detects the prompt gamma rays from the top-side of the sample. The moderator is placed adjacent to the neutron target plane of the portable neutron generator. In order to prevent undesired gamma-rays and neutrons from reaching

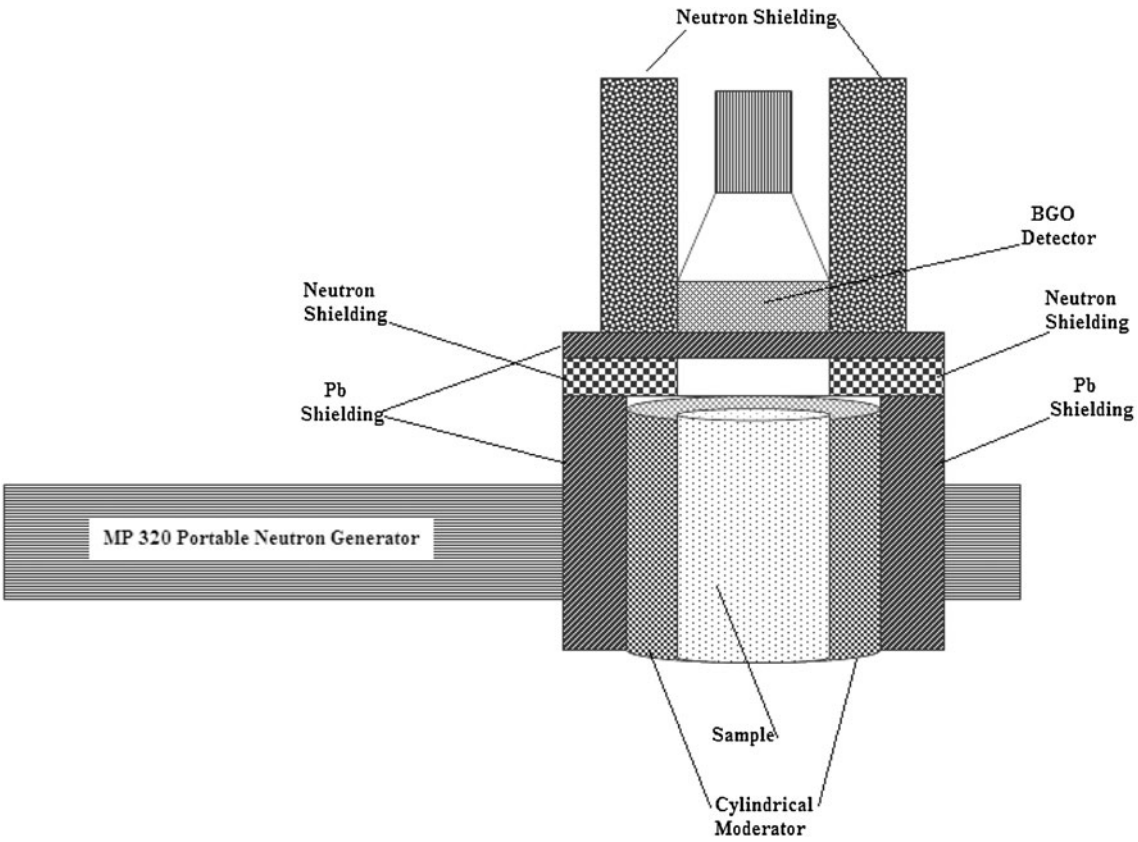

Fig. 3 Schematic side view of the portable neutron generator based optimized PGNAA setup

the detector, 3 mm thick lead shielding and 50 mm thick neutron shielding are surrounding the gamma-ray detector. The neutron shielding is made of a mixture of paraffin and lithium carbonate mixed in equal weight proportions.

In the next step the prompt gamma-ray count rates of mercury were calculated from water samples contained in 90 mm diameter and 145 mm long plastic bottles. The water samples were prepared by mixing mercury salt with water in 1.25, 2.50, 5.00, and 10.0 wt% mercury proportions. The count rates of 2.64, 3.19 + 3.29, and 4.67–5.05 MeV Hg prompt gamma-rays were calculated for different Hg concentrations in the water samples. The intensities and energies of various Hg prompt gamma ray lines due to thermal neutron capture in Hg are given in Table 1 [15].

Table 1 Energies and production cross section $\sigma_{\gamma}^{z}(E_{\gamma})$ barns of prominent capture gamma-rays of bismuth, germanium and mercury [15]

Element	Gamma-ray energy (keV)	$\sigma_{\gamma}^{z}(E_{\gamma})$ (barns)
Bi	162	0.008
	320	0.0115
	674	0.0026
	2,505	0.0021
	2,828	0.00179
	4,054	0.0137
	4,171	0.0171
Ge	175	0.164
	493	0.133
	500	0.162
	596	1.100
	608	0.250
	868	0.553
	961	0.129
	1,101	0.134
	1,204	0.141
	1,472	0.083
Hg	368	251
	1,570	29.6
	1,693	56.2
	2,002	24.3
	2,639	11.6
	3,186	11.3
	3,289	13.3
	4,675	13
	4,739	30
	4,759	12.5
	4,842	20
	5,050	20
	5,658	27.5
	5,967	62.5
	6,458	23

The efficiency calibration curve obtained by the analysis of standard solutions spiked with known amount of Hg was used to calculate mercury in contaminated water samples.

Prompt gamma-ray analysis of Hg-contaminated Water samples

Four Hg-contaminated water samples with 1.25, 2.50, 5.00, and 10.0 wt% Hg concentrations were prepared. The water samples were then irradiated in the newly designed MP320 generator-based PGNAA setup. A pulsed beam of 2.5 MeV neutrons was produced with 70 keV deuteron beam via D(d,n). The deuteron pulse had a width of 5 ms and a frequency of 250 Hz. The pulsed neutron beam improved the signal to background ratio in the PGNAA studies. A typical beam current of the generator was 70 μÅ. The prompt gamma-ray data from Hg-contaminated water samples were acquired using a cylindrical 125 × 125 mm (diameter × height) BGO detector for 25 min. Due to its radiation resistant property against neutron damage, BGO was selected as a gamma ray detector. During irradiation of the samples, the BGO detector, although well shielded, was also exposed to thermal neutrons and it registered the prompt gamma-rays due to the capture of thermal neutrons in Bi and Ge elements present in the BGO detector. There might be interferences from other elements present in the environmental sample in this energy but due to large thermal capture cross section of Hg, very small contamination of Hg will be still detectable in spite of those interferences. The energies and intensities of prominent prompt gamma-rays due to capture of thermal neutrons in detector material and Hg are listed in Table 1 [15].

Results and discussion

Figures 4, 5, 6 show the pulse height spectra of the BGO detector from water samples contaminated with mercury. Figure 4 shows the pulse height spectra of prompt gamma-rays from water samples containing 1.25, 2.50, 5.00, and 10.0 wt% Hg concentrations superimposed upon each other along with the background spectrum taken with non-contaminated demineralized water sample. Figure 4 also shows the 2.22 MeV hydrogen capture peak from the moderator material along with 2.64, 3.19 + 3.29, and 4.67–5.05 MeV prompt gamma ray peaks from mercury in the contaminated water. Moreover, Fig. 4 also shows unresolved prompt gamma ray peaks at 4.06–4.25 MeV energies from bismuth in BGO detector material. The BGO detector has poor energy resolution (11 % for 662 keV gamma-rays from ^{137}Cs source).

Figure 5 shows enlarged prompt gamma rays pulse height spectra of the four Hg-contaminated water samples

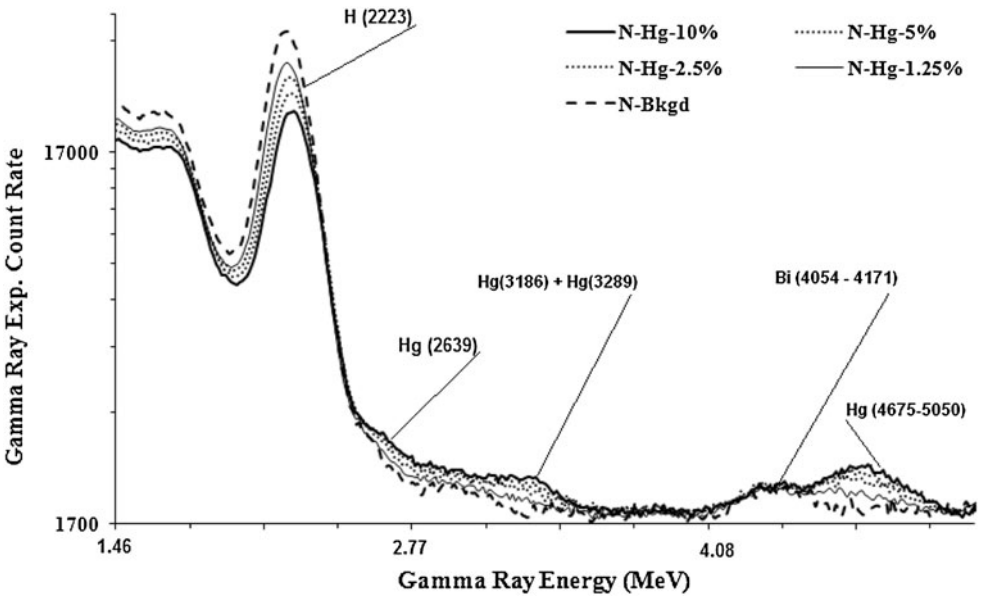

Fig. 4 Prompt gamma-ray experimental pulse height spectra from mercury contaminated water sample containing 1.25, 2.50, 5.00, and 10.0 wt% mercury showing 2.64, 3.19 + 3.29, and 4.67–5.05 MeV prompt gamma rays peaks of mercury also superimposed is the background gamma-ray spectrum

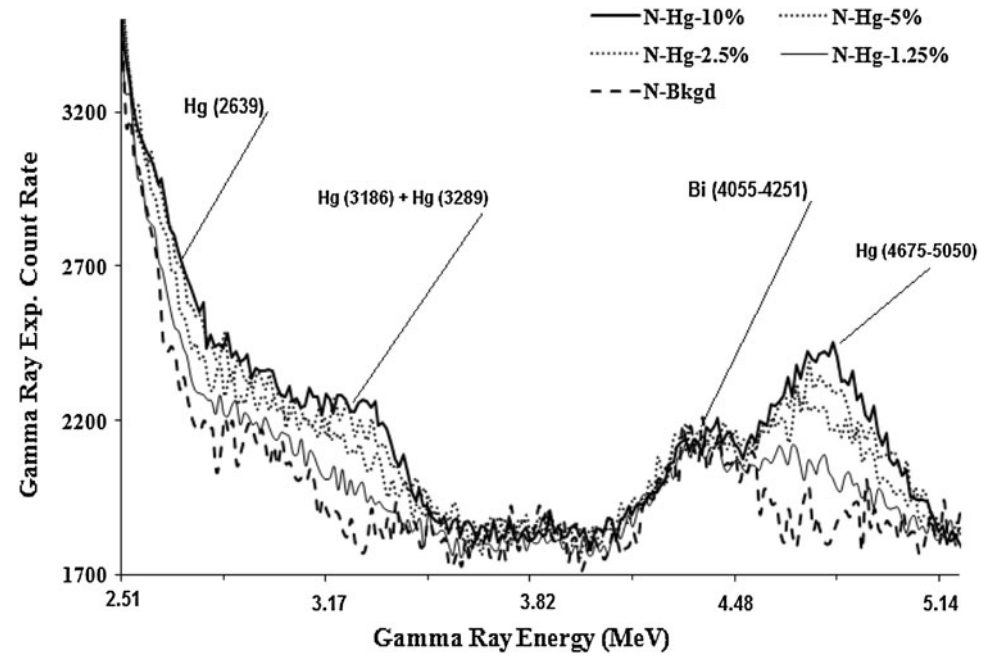

Fig. 5 Enlarged prompt gamma-ray experimental pulse height spectra from 1.25, 2.50, 5.00, and 10.0 wt% mercury contaminated water sample over 2.51–5.14 MeV showing 2.64, 3.19 + 3.29, and 4.67–5.05 MeV prompt gamma rays peaks of mercury

over 2.51–5.14 MeV gamma energy range, showing an increase in intensity of 2.64, 3.19 + 3.29, and 4.67–5.05 MeV Hg prompt gamma ray peaks with increasing Hg concentration in the water samples. Figure 6 shows the difference spectra showing well resolved peaks of 2.64, 3.19 + 3.29, and 4.67–5.05 MeV prompt gamma rays of Hg for the four samples containing 1.25, 2.50, 5.00, and 10.0 wt% Hg concentrations. These spectra were obtained after subtracting the background spectrum from each sample pulse height spectrum.

Finally, the peaks of the difference spectra were integrated to generate integrated count rates of 2.64, 3.19 + 3.29, and 4.67–5.05 MeV prompt gamma ray peaks of Hg as a function of mercury concentration, as shown in Fig. 7. The solid line in Fig. 7 represents the results obtained from Monte Carlo calculations following the procedure described elsewhere [5]. Each gamma ray line has different slope of count rate versus Hg-concentration. The slope of the line defines minimum detectable activity (MDA) of the PGNAA setup for the specific element using that particular gamma line. The maximum value of slope of count rate versus Hg-concentration observed in the present study is for the 4.67–5.05 MeV line. The MDA of Hg for high energy gamma rays studied in this study is expected to be

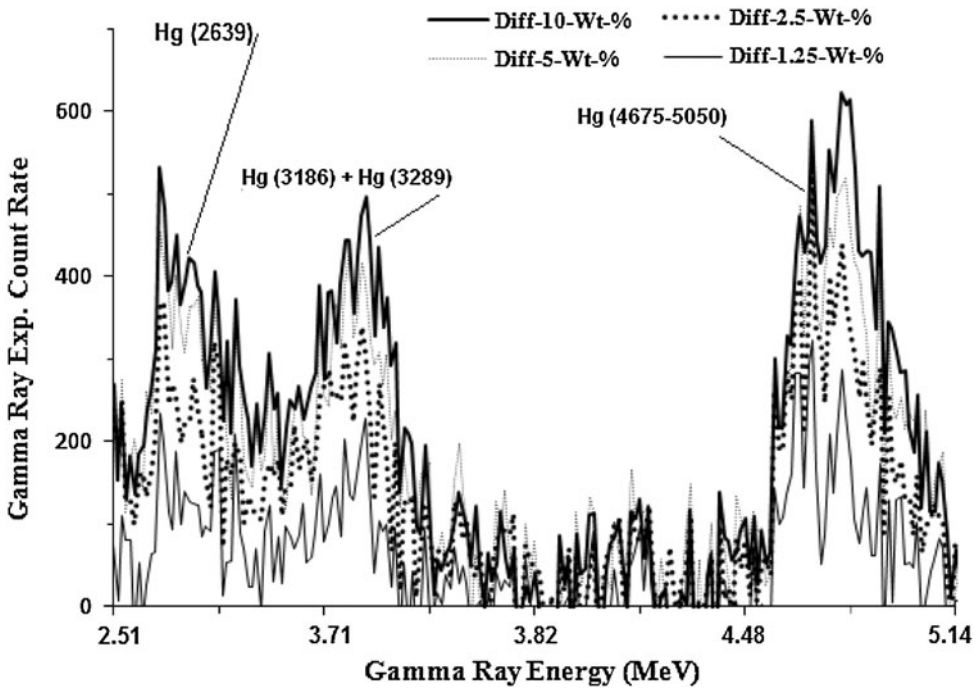

Fig. 6 Enlarged mercury prompt gamma-ray pulse height difference spectra for water sample containing 0.625, 1.25, 2.50, 5.00, and 10.0 wt% mercury after background subtraction over 2.51–5.14 MeV and showing 2.64, 3.19 + 3.29, and 4.67–5.05 MeV mercury peaks

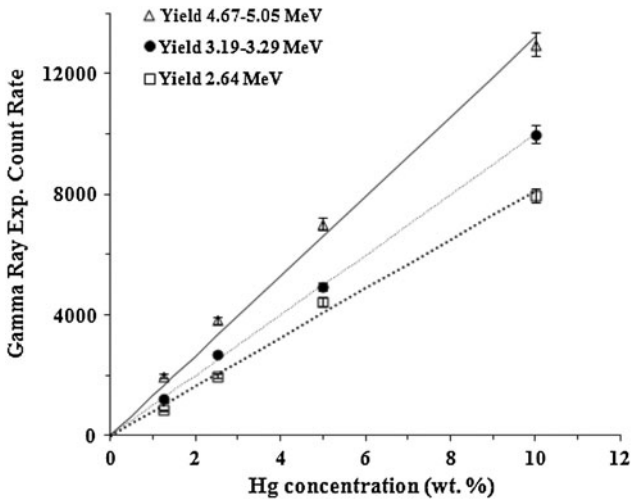

Fig. 7 Experimental integrated count rate of 2.64, 3.19 + 3.29, and 4.67–5.05 MeV prompt gamma-rays from mercury plotted as a function of mercury concentration in water samples. *Line* represents the results of the Monte Carlo simulations

quite poor as compared to that obtained using high-intensity, low-energy 386 keV Hg gamma ray. The MDA of Hg using 2.5–5.1 MeV gamma rays for the portable neutron generator based PGNAA setup was calculated to be 0.19 ± 0.06 wt%. For 386 keV Hg gamma ray, with two order of magnitude larger production cross section, the corresponding MDA is expected to be about 19 ppm. There is an excellent agreement between the theoretical count rate and the experimental count rate of prompt gamma-rays from mercury measured by a BGO detector as a function of Hg concentration in the water samples.

Conclusions

In this study a portable neutron generator-based PGNAA set up has been designed and tested for analysis of bulk environmental samples. The PGNAA set up response was tested through prompt gamma ray count rate measurements from water samples containing 1.25, 2.50, 5.00, and 10.0 wt% Hg concentrations using 2.64, 3.19 + 3.29, and 4.67–5.05 MeV prompt gamma ray peaks of Hg. An excellent agreement has been observed between the experimental and calculated count rates of prompt gamma-rays for the given mercury concentrations. This indicates the excellent performance of the portable neutron generator based PGNAA set up for the analysis of environmental samples.

Acknowledgments This study is part of a Project # RG1201 funded by the King Fahd University of Petroleum and Minerals, Dhahran, Saudi Arabia. The support provided by the Department of Physics, Department of Chemistry and Energy Research Center, King Fahd University of Petroleum and Minerals, Dhahran, Saudi Arabia, is also acknowledged.

References

1. Dulloo AR, Hruddy F, Congedo TV, Gseidel J, Gehrke RJ (1998) Nucl Technol 123:103
2. Grinyer J, Byun SH, Chettle DR (2005) Appl Radiat Isot 63:475
3. Howell SL, Sigg RA, Moore FS, Devolj TA (2000) J Radioanal Nucl Chem 244:173
4. Idiri Z, Mazrou H, Amokrane A, Bedek S (2010) Nucl Instrum Methods Phys Res B26(8):213
5. Naqvi AA, Al-Anezi MS, Zameer Kalakada, Isab AA, Raashid M, Al Matouq FA, Khateeb-Ur-Rehman, Khiari FZ, Garwan MA,

Al-Amoudi OSB, Maslehuddin M (2011) Nucl Instrum Methods Phys Res A 665:74
6. Livingston RA, Al-Sheikhl YM, Ali BM (2010) Appl Radiat Isot 68:679
7. Eleon C, Perot B, Carasco C, Sudac D, Obhodas J, Valkovic V (2011) Nucl Instrum Methods Phys Res 629:220
8. Chichester DL, Simpson JD, Lemchak M (2007) J Radioanal Nucl Chem 271:629
9. Hamid A, Hassan AM (2012) J Radioanal Nucl Chem 291(3): 617–621
10. Ghorbani P, Sardari D, Bayat E, Mahammadi VD (2012) J Radioanal Nucl Chem 291(3):839–842
11. Horne S, Landesberger S (2012) J Radioanal Nucl Chem 291(1): 49–53
12. Rios Perez CA et al (2012) J Radioanal Nucl Chem 291(1): 261–265
13. Fantidis JG et al (2011) J Radioanal Nucl Chem 290(2):289–295
14. Briesmeister JF (ed) (1997) Los Alamos National Laboratory Report LA-12625-M 4A
15. Choi HD, Firestone RB, Lindstrom RM, Molnar GL, Mughabghab SF, Paviotti-Corcuera R, Revay ZS, Trkov A, Zhou CM (2006) International Atomic Energy Agency, Vienna